

# Stability of 1-D Excitons in Carbon Nanotubes under High Laser Excitations

G. N. Ostojic, S. Zaric, and J. Kono\*

*Department of Electrical and Computer Engineering, Rice Quantum Institute,  
and Center for Nanoscale Science and Technology, Rice University, Houston, Texas 77005*

V. C. Moore, R. H. Hauge, and R. E. Smalley

*Department of Chemistry, Rice Quantum Institute,  
and Center for Nanoscale Science and Technology, Rice University, Houston, Texas 77005*

(Dated: September 13, 2018)

Through ultrafast pump-probe spectroscopy with intense pump pulses and a wide continuum probe, we show that interband exciton peaks in single-walled carbon nanotubes (SWNTs) are extremely stable under high laser excitations. Estimates of the initial densities of excitons from the excitation conditions, combined with recent theoretical calculations of exciton Bohr radii for SWNTs, suggest that their positions do not change at all even near the Mott density. In addition, we found that the presence of lowest-subband excitons broadens all absorption peaks, including those in the second-subband range, which provides a consistent explanation for the complex spectral dependence of pump-probe signals reported for SWNTs.

Optically-excited electron-hole ( $e-h$ ) pairs in a semiconductor provide a rich system for the study of carrier interaction effects. Depending on the density, they exhibit qualitatively different spectral features of bound and unbound carriers. Excitons (or bound  $e-h$  pairs) are stable when the Bohr radius is much smaller than the inter-exciton distance. As the former approaches the latter, the Mott transition [1] occurs, transforming the insulating excitonic gas into a metallic  $e-h$  plasma. This scenario is complicated in real systems by other interaction effects such as band gap renormalization (BGR) and biexcitonic correlations. In addition, optical gain develops and coherent processes can dominate the emission spectra. There have been a number of studies on highly-excited 3-D and 2-D semiconductor systems [2, 3].

1-D excitons are expected to be different: the exciton binding energy in an ideal 1-D system is infinite [4], the 1-D Sommerfeld factor is less than 1 [5], and radiative lifetimes are intrinsically longer [6]. High-density excitons in semiconductor quantum wires [7, 8, 9, 10, 11] have exhibited a range of novel (and conflicting) results regarding gain, BGR, and Mott transitions. The magnitude of 1-D BGR is still under debate, but it appears to be a common observation that 1-D excitons are stable up to very high densities [8, 9, 10]. This stability, while good for device applications, is not fully understood, and the density at which gain should appear is a subject of controversy [12].

Excitons in carbon nanotubes can provide new insight into these long-standing issues. With much smaller diameters (and thus larger subband separations and binding energies), these excitons should allow one to study high-density regimes without having to take into account the population of higher subbands. Since the success of preparing individually-suspended single-walled carbon nanotubes (SWNTs) [13, 14], their optical properties have been intensively studied. While theoretical

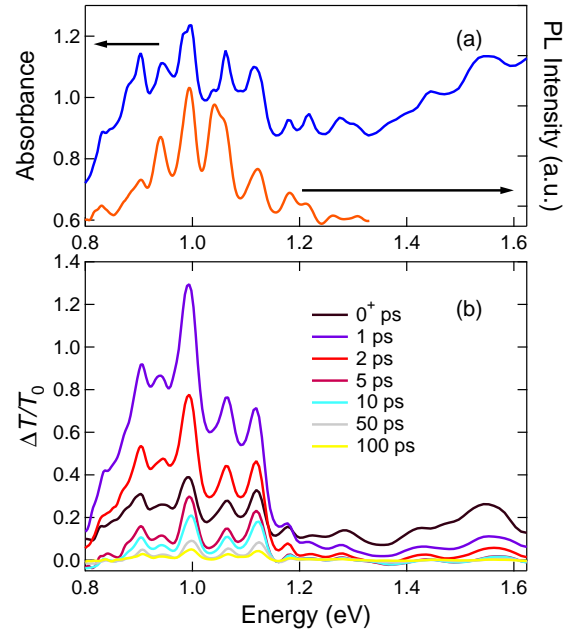


FIG. 1: (a) Linear absorption (blue line, left axis) and PL (red line, right axis) spectra. The PL was taken with CW 1.6 eV (775 nm) excitation. (b) Chirp corrected differential transmission spectra for various time delays.

understanding of linear optical properties is progressing [15, 16, 17, 18, 19, 20], their nonlinear optical properties, especially under high excitations, remain unexplored. Recent time-resolved studies on bundled [21, 22] and unbundled [23, 24, 25, 26, 27] SWNTs have raised an array of questions on the origin of non-radiative recombination and the values of intrinsic radiative lifetimes. In particular, strongly wavelength-dependent non-degenerate pump-probe data [21, 22, 24] have produced differing interpretations.

In this Letter, we report results of non-degenerate

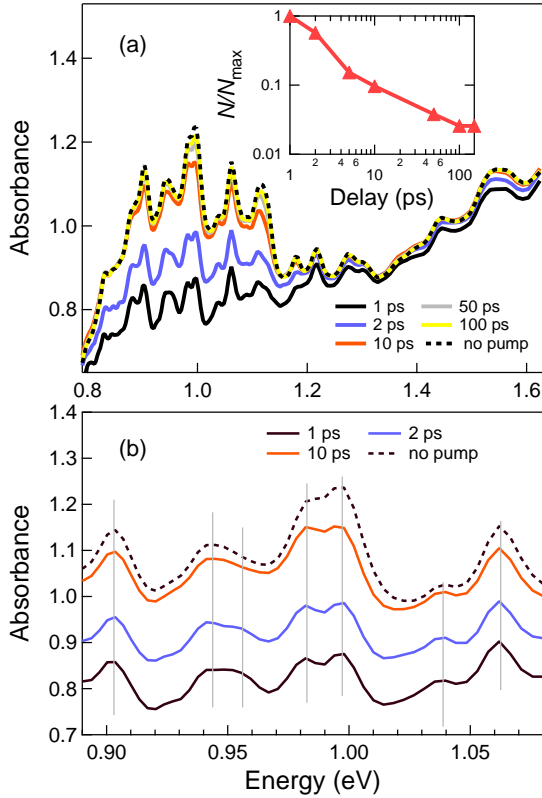


FIG. 2: (a) Absorbance spectra at different time delays, reconstructed from the differential transmission data in Fig. 1. The inset shows the time decay of the normalized  $e$ - $h$  pair density, obtained by spectrally integrating the absorbance change at each time delay. (b) Absorbance spectra within the first subband range at different time delays, showing that exciton peaks do not shift.

pump-probe spectroscopy with a strong pump beam and a white-light continuum probe. From excitation conditions we estimated the initial pair density to be  $\sim 5 \times 10^6 \text{ cm}^{-1}$ . This, combined with recent calculations of the Bohr radius (2-5 nm) [17, 18, 19], indicates that the initial density is comparable to the Mott density. However, the band edge absorption peaks were very stable, their positions showing no variation with time (i.e., density), similar to the observations in quantum wires [8, 9, 10]. Furthermore, we found that there are long-lived (up to  $\sim 100$  ps), pump-probe signals in the second-subband transition range, even though there are no real carriers left. Through spectral analysis we concluded that the absorption peaks are broadened by the excitons present in the first subbands. This result provides a new and consistent scenario for the complex pump-probe dynamics.

The samples used in our experiments were micelle-suspended in  $\text{D}_2\text{O}$ , which showed a number of chirality-dependent peaks in photoluminescence (PL) and absorption [13]. The first ( $E_{11}$ ) and second ( $E_{22}$ ) subband transition energies were determined through PL excitation

(PLE) spectroscopy. They possess long pump-probe decay times, especially when excited resonantly [23]. Similar lifetimes have been reported using time-resolved PL measurements [24, 25, 26], indicating that these long lifetimes are related to radiative interband recombination.

We used an optical parametric amplifier (OPA) pumped by a chirped-pulse amplifier (CPA2010, Clark-MXR) that produced 150-fs pulses at 1 kHz. As a pump, either the OPA beam covering 0.07–2.5 eV or the CPA beam (1.6 eV or 775 nm) was used. Pump fluences up to  $\sim 1 \text{ mJ/cm}^2$  were used. As a probe, we used a white light continuum generated by focusing a small portion of the CPA beam onto a sapphire crystal, covering wavelengths from the visible to the infrared. Both beams were focused onto a 5-mm thick sample cell with pump and probe diameters 1 mm and 0.8 mm, respectively. After passing through the sample, the probe was spectrally resolved with a monochromator and detected by an InGaAs photodiode. Chirp in the probe was measured through a second harmonic generation technique, and it was taken into account in all data analysis. The pulse width of the probe (i.e., the temporal resolution of the setup) was 270 fs. To detect the small change in probe transmission  $\Delta T$ , we synchronously chopped the pump beam at 500 Hz, which blocked every other pump pulses. The probe pulse train was then sampled in a box car integrator that electronically inverted every other signals. A computer then collected the pulses and separate them to extract pump influenced ( $T$ ) and non-influenced transmission ( $T_0$ ).

Absorption and PL spectra are shown in Fig. 1(a). The PL was excited by CW 775 nm radiation. Differential transmission spectra with a 775 nm pump are shown in Fig. 1(b) for different time delays. At 0 ps, positive  $\Delta T$  exists both in the  $E_{11}$  and  $E_{22}$  ranges. However, during the first 1 ps, the signal in the  $E_{11}$  range rapidly increases at the expense of the signal in the  $E_{22}$  range, indicating a fast intraband (i.e., intersubband) carrier decay. At subsequent time delays, the overall shape of the spectra remains the same, and the amplitude decays slowly.

The evolution of absorbance, obtained from differential transmission, is shown in Fig. 2(a). Absorption quenching up to  $\sim 80\%$  is seen at 1 ps but it recovers as time progresses. At 100 ps, the absorption spectrum coincides with that taken at negative time delays, indicating that a majority of carriers have already recombined. The inset shows the estimated pair density versus time, normalized to the value at 1 ps. The density at each time delay was deduced from the amount of spectrally-integrated absorption change. Figure 2(b) shows an expanded view in the 0.9–1.1 eV range. It is seen that the *absorption peak positions do not change at all with time, i.e., with density*, while linewidths increase slightly.

We also found that the presence of first subband excitons modifies the absorption in the second subband. Figure 3(a) shows  $\Delta T/T_0$  as a function of probe energy, mostly in the second subband range. This continuous

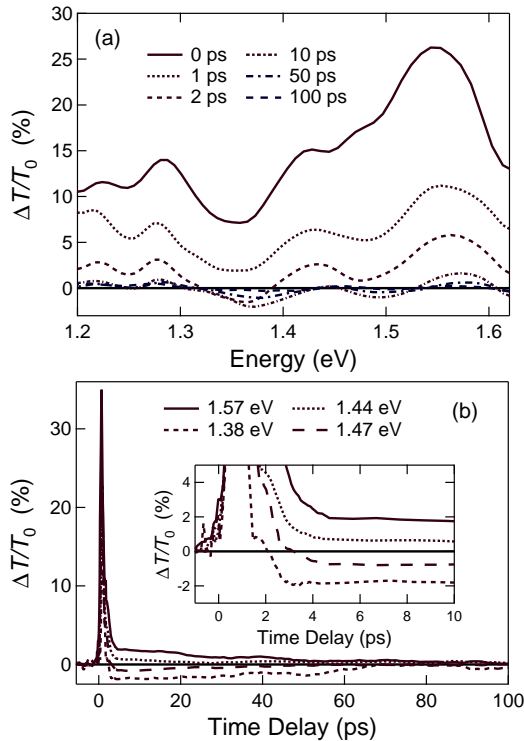


FIG. 3: (a) Differential transmission spectra at different time delays in the second subband range. (b) Differential transmission dynamics at four different probe photon energies. At some probe photon energies the signal becomes negative (corresponding to absorption increase).

probing reveals previously-unobserved *oscillatory behavior*. Especially after 1 ps, when all carriers have decayed into the first subband, the *sign of  $\Delta T$  sensitively depends on the probe energy*. Positive  $\Delta T$  (i.e., absorption bleaching) is located mostly around absorption peaks while negative  $\Delta T$  (i.e., photoinduced absorption) exists in the vicinity of absorption dips. Examples of  $\Delta T/T_0$  versus time delay for selected probe energies are shown in Fig. 3(b). Upon close examination, this oscillatory behavior is also seen in the first subband range, superimposed onto the positive band filling signal.

The density of photo-excited  $e$ - $h$  pairs ( $n_X$ ) was estimated as follows. For typical 1-nm-diameter nanotubes that are abundant in the sample [say, (8,7) tubes], the linear mass density is calculated to be  $2.4 \times 10^{-11}$  mg/cm. This, combined with the mass density (52.4 mg/l from linear absorption with Beer's law) and the average tube length (150 nm from atomic force microscopy), provides  $5.7 \times 10^{11}$  as the total number of tubes within the pump-excited volume ( $3.9 \text{ mm}^3$ ). The number of absorbed photons (and thus created  $e$ - $h$  pairs) in the same volume is estimated to be  $2.1 \times 10^{13}$  from the nonlinear absorbance (1.043 at 0 ps for 1.6 eV) and the pump energy ( $12 \text{ } \mu\text{J}$ ). These numbers yield  $n_X \approx 5 \times 10^6 \text{ cm}^{-1}$  (or an average separation of  $\sim 2 \text{ nm}$ ). [Note that the average length

(150 nm) cancels out and does not affect  $n_X$ .] A possible source of uncertainty in  $n_X$  is the existence of residual bundles, which can absorb the pump and make the estimated  $n_X$  larger. However, the clear appearance of peaks in absorption indicates that absorption from unbundled SWNTs is dominant. A possible error may also come from the neglect of scattering, but a recent study [28] indicates that scattering is of small importance for low repetition-rate femtosecond pulses. Finally, we did not take into account any contribution of two-photon absorption, which should lead to the creation of  $e$ - $h$  pairs at 3.2 eV, mostly in metallic nanotubes, and thus reduce the pair density in semiconductor nanotubes.

Recent theoretical calculations using different methods [17, 18, 19] have reported 2-5 nm for the Bohr radii ( $a_B^*$ ) of excitons in SWNTs with a  $\sim 1 \text{ nm}$  diameter. This suggests that  $r_s = n_X a_B^* \sim 1$ . Namely, right after they are created by the pump pulse, the exciton density is similar to the 1-D Mott density. Since the photoinduced carrier density decays to almost zero in  $\sim 200 \text{ ps}$ , this translates that we are monitoring the behavior of exciton peaks in a widely varying density range, going from the initial high-density regime to the final dilute limit. Nonetheless, the observed absorption peaks are very stable in position. This stability is similar to what has been observed in high-quality GaAs quantum wires [8, 9, 10], implying a unique nature of excitons in 1-D systems.

Previous pump-probe spectroscopy studies on bundled nanotubes [21, 22] exhibited similar probe-energy-dependent bleaching and absorption behaviors, but different mechanisms were proposed. Lauret *et al.* [21] created carriers in the first subband and observed increased absorption at selected probe energies, which was interpreted as a redshift of the “plasmon” absorption peak. Korovyanko *et al.* [22] explored various probe energies and concluded that a global red shift is not a consistent picture to explain their data; instead they attributed the photoinduced absorption observed at some probe energies to excitonic intersubband transitions. Neither of the proposed mechanisms can explain our data. Since our sample consists of unbundled SWNTs that exhibit chirality-dependent peaks, we can readily see that we have no global red shift or photo-induced absorption peaks corresponding to intersubband-like transitions.

We believe that the probe-energy-dependent sign of differential transmission can be consistently explained in terms of carrier-induced peak broadenings. Figure 4(a) depicts the idea, which is a simulation result based on three Lorentzian peaks. All three tube types are assumed to have a half-width at half maximum of 8 meV and one of them is assumed to have a larger amplitude. It can be seen that the sign of pump-probe signal should show the observed oscillatory behavior. It can also be seen that the change of a small peak can be significantly influenced by a neighboring large peak. Figure 4(b) is a simulation result based on a global red shift; this model fails to

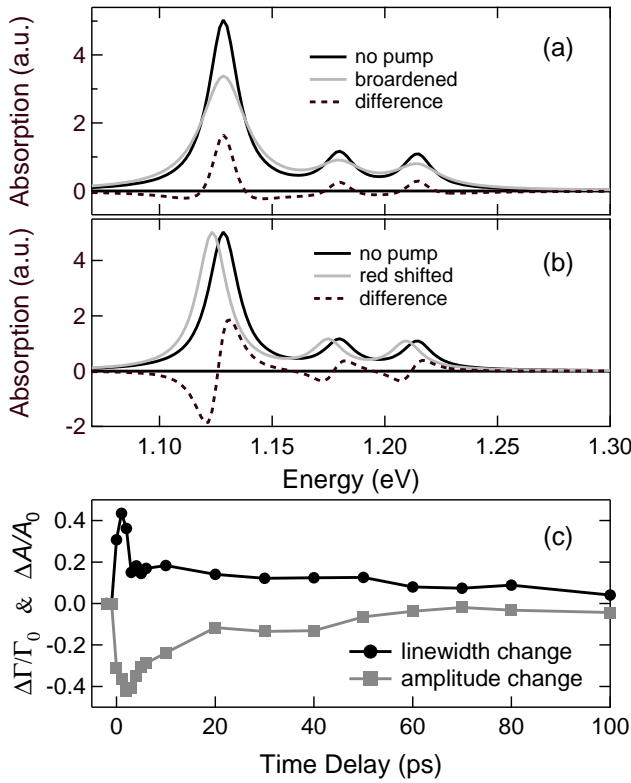


FIG. 4: Simulated differential absorption spectra for three closely-lying lines with different amplitudes based on (a) line broadening and (b) a rigid red shift. (c) Obtained best fit Lorentzian parameters for the 1.17 eV absorption peak of (10,2) nanotubes.

explain any of the observed features.

To analyze the photoinduced broadening in more detail, we concentrated on (10,2) tubes, which have an  $E_{11}$  peak reasonably separated from other tubes and is relatively weakly populated (i.e., the positive band filling signal is small). The evolution of the extracted Lorentzian parameters (peak amplitude  $\Delta A/A_0$  and linewidth  $\Delta\Gamma/\Gamma_0$ ) normalized to the negative delay values are shown in Fig. 4(c). Broadening and amplitude change follow the fast rise seen in  $\Delta T/T_0$ . However, the subsequent decay is slightly faster for the broadening. The amplitude decay is related to state filling but also can result from the screening of the Coulomb interaction. The latter effect produces broadening although carrier-phonon scattering and carrier-carrier scattering can have important roles in broadening in the regime of high carrier density, which could explain the faster decay of broadening compared to the amplitude change.

In conclusion, we have performed non-degenerate

pump-probe spectroscopy on micelle-suspended SWNTs and found 1) that interband exciton peaks are very stable even at very high densities and 2) that second-subband absorption peaks are broadened by the excitons present in the first subbands, which provides a new and consistent explanation for the complex behavior of pump-probe signals reported for bundled and unbundled SWNTs.

We gratefully acknowledge support from the Robert A. Welch Foundation (Grant No. C-1509), the Texas Advanced Technology Program (Project No. 003604-0001-2001), and the National Science Foundation (Grant Nos. DMR-0134058 and DMR-0325474).

\* To whom correspondence should be addressed; URL: <http://www.ece.rice.edu/~kono>; Electronic address: kono@rice.edu

- [1] N. F. Mott, Phil. Mag. **6**, 287 (1961).
- [2] H. Haken and S. Nikitine, eds., *Excitons at High Density* (Springer-Verlag, Berlin, 1975).
- [3] H. Haug and S. W. Koch, *Quantum Theory of the Optical and Electronic Properties of Semiconductors, Fourth Edition* (World Scientific, Singapore, 2004).
- [4] R. Loudon, Am. J. Phys. **27**, 649 (1959).
- [5] T. Ogawa and T. Takagahara, Phys. Rev. B **43**, 14325 (1991); *ibid.* **44**, 8138 (1991).
- [6] D. S. Citrin, Phys. Rev. Lett. **69**, 3393 (1992).
- [7] E. Kapon *et al.*, Phys. Rev. Lett. **63**, 430 (1989).
- [8] W. Wegscheider *et al.*, Phys. Rev. Lett. **71**, 4071 (1993).
- [9] R. Ambigapathy *et al.*, Phys. Rev. Lett. **78**, 3579 (1997).
- [10] H. Akiyama *et al.*, Solid State Commun. **122**, 169 (2002).
- [11] H. Akiyama *et al.*, Phys. Rev. B **67**, 041302 (2003).
- [12] F. Rossi and E. Molinari, Phys. Rev. Lett. **76**, 3642 (1996); F. Tassone and C. Piermarocchi, Phys. Rev. Lett. **82**, 843 (1999); S. Das Sarma and D. W. Wang, Phys. Rev. Lett. **84**, 2010 (2000).
- [13] M. J. O'Connell *et al.*, Science **297**, 593 (2002).
- [14] S. M. Bachilo *et al.*, Science **298**, 2361 (2002).
- [15] T. Ando, J. Phys. Soc. Jpn. **66**, 1066 (1997).
- [16] C. L. Kane and E. J. Mele, Phys. Rev. Lett. **90**, 207401 (2003).
- [17] C. D. Spataru *et al.*, Phys. Rev. Lett. **92**, 077402 (2004).
- [18] E. Chang *et al.*, Phys. Rev. Lett. **92**, 196401 (2004).
- [19] T. G. Pederson, Carbon **42**, 1007 (2004).
- [20] V. Perebeinos *et al.*, Phys. Rev. Lett. **92**, 257402 (2004).
- [21] J. S. Lauret *et al.*, Phys. Rev. Lett. **90**, 057404 (2003).
- [22] O. J. Korovyanko *et al.*, Phys. Rev. Lett. **92**, 017403 (2004).
- [23] G. N. Ostojic *et al.*, Phys. Rev. Lett. **92**, 117402 (2004).
- [24] Y.-Z. Ma *et al.*, J. Chem. Phys. **120**, 3368 (2004).
- [25] A. Hagen *et al.*, Appl. Phys. A **78**, 1137 (2004).
- [26] F. Wang *et al.*, Phys. Rev. Lett. **92**, 177402 (2004).
- [27] L. Huang *et al.*, Phys. Rev. Lett. **93**, 017403 (2004).
- [28] L. Vivien *et al.*, Carbon **40**, 1789 (2002).